Journal of Molecular Structure 1322 (2025) 140241

Contents lists available at ScienceDirect

Journal of Molecular Structure

journal homepage: www.elsevier.com/locate/molstr

A new Schiff-base complex of palladium nanoparticles on modified Fe_3O_4 with 3,5-diaminobenzoic acid (DAA) as a robust, reusable, and selective catalyst in the C—N and C—C coupling reactions

Durgesh Singh [a,*], Kamini Singh [b], Vicky Jain [c], Subbulakshmi Ganesan [d], Junainah Abd Hamid [e], Mamata Chahar [f], Suman Saini [g], Munther Kadhim Abosaoda [h,i], M. Atif [j], Mohammed A. El-Meligy [k,l]

[a] Department of Chemistry,School of Chemical Sciences and Technology, Dr.Harisingh Gour Vishwavidyalaya (A Central University), Sagar - 470003, India
[b] Department of Chemistry, Deen Dayal Upadhyay Gorakhpur University, Gorakhpur 273009, India
[c] Marwadi University Research Center, Department of Chemistry, Faculty of Science Marwadi University, Rajkot-360003, Gujarat, India
[d] Department of Chemistry and Biochemistry, School of Sciences, JAIN (Deemed to be University), Bangalore, Karnataka, India
[e] Management and Science University, Shah Alam, Selangor, Malaysia
[f] Department of Chemistry, NIMS Institute of Engineering & Technology, NIMS University Rajasthan, Jaipur, India
[g] Department of Applied Sciences, Chandigarh Engineering College, Chandigarh Group of Colleges-Jhanjeri, Mohali 140307, Punjab, India
[h] College of pharmacy, the Islamic University, Najaf, Iraq
[i] College of pharmacy, the Islamic University of Al Diwaniyah, Al Diwaniyah, Iraq
[j] Department of Physics and Astronomy, College of Science, King Saud University, P O Box 2455, Riyadh 11451, Saudi Arabia
[k] Jadara University Research Center, Jadara University, PO Box 733, Irbid, Jordan
[l] Applied Science Research Center, Applied Science Private University, Amman, Jordan

ARTICLE INFO

Keywords:
Schiff base
Complex
Cross-coupling
Nanoparticles
Fe_3O_4

ABSTRACT

A Pd Schiff base complex was immobilized onto the surface of magnetic Fe_3O_4 as a novel, green, and recyclable heterogeneous nanocatalyst and fully characterized by TEM, XRD, FT-IR, BET, SEM, ICP-OES, EDS, TGA, and VSM techniques. The Fe_3O_4@SiO_2@DAA@Schiff base-Pd(0) catalyst exhibits outstanding performance in catalyzing Buchwald-Hartwig and Stille coupling reactions, resulting in high yields of the corresponding products. This catalyst offers numerous benefits, such as a straightforward testing procedure, environmentally friendly reaction conditions, absence of hazardous solvents, quick reaction time, low catalyst usage, and the ability to be reused. Furthermore, the nanocatalyst could be effortlessly separated from the reaction mixture using a bar magnet, enabling its repeated recovery and reuse without compromising its stability or activity.

1. Introduction

In the past ten years, one noteworthy achievement by scientists has been the identification of the Suzuki reaction in the presence of palladium metal complexes [1]. The Stille reaction, which involves coupling triphenyltin chloride and aryl halide, is commonly employed as a straightforward and effective method for synthesizing biphenyls [2,3]. Transition metal catalyst systems have sparked a revolution in synthetic methodologies for creating organic compounds through carbon-heteroatom and carbon-carbon coupling reactions [4–7]. These model reactions are commonly utilized in the production of pharmaceuticals, agricultural products, and various chemical compounds [8–15]. Aromatic amines are commonly found in a wide range of synthetic and natural products, such as agricultural and pharmaceutical chemicals, medications, fragrances, and flavorings [16,17]. The creation of synthetic protocols for C—N bonds has been significantly important across various industries and academic fields [18]. The Buchwald-Hartwig reaction is a valuable catalytic method promoted by transition metals for forming C—N bonds [19].

The development and research of new and efficient nanocatalysts as catalyst support is a big challenge in the synthesis of organic compounds [20,21]. Over the past ten years, magnetic nanoparticles have become widely utilized as supports in the fabrication of magnetic nanocatalysts, owing to their straightforward preparation and convenient retrieval

* Corresponding author.
E-mail address: durgesh.phdchem16@gmail.com (D. Singh).

https://doi.org/10.1016/j.molstruc.2024.140241
Received 18 July 2024; Received in revised form 16 September 2024; Accepted 29 September 2024
Available online 1 October 2024

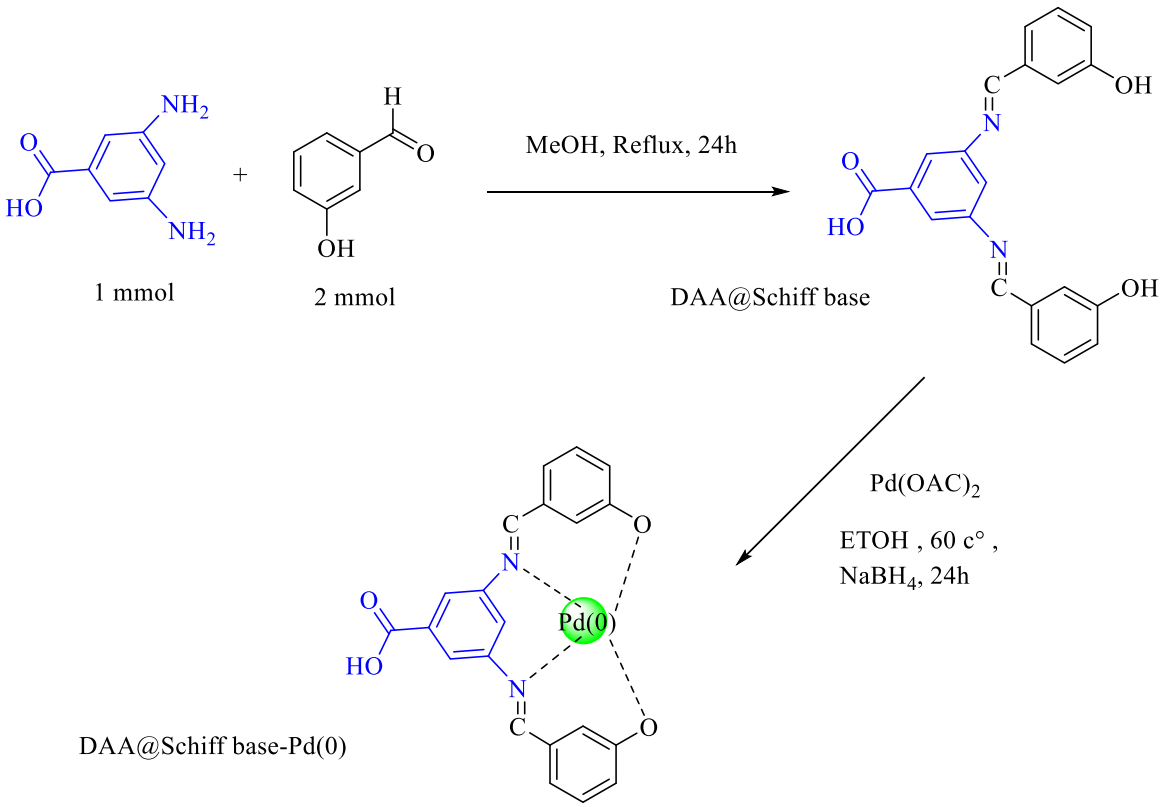

Scheme 1. Preparation of DAA@Schiff base-Pd(0).

using a magnetic field. One of the benefits of magnetic nanoparticles is the ease with which they can be separated from the reaction mixture using an external magnet. Fe_3O_4 is widely favored as a heterogeneous catalyst due to its simple synthesis and the ease with which its surface can be modified using a magnet. Different catalysts can be supported on Fe_3O_4 nanoparticles due to easy separation after several reuses. In this project, we report the synthesis and characterization of a new and green nanocatalyst with Pd ion stabilization and investigate their application as a amide catalyst in C—N and C—C cross-coupling reactions.

2. Experimental

2.1. Synthesis of DAA@Schiff base-Pd(0)

In a round-bottomed balloon, a mixture of 3,5-Diaminobenzoic acid (1.0 mmol) was added to 3-Hydroxybenzaldehyde (2.0 mmol) in Methanol (10 mL) mixture and stirred under reflux conditions for 24 h. The reaction mixture turned yellow due to the formation of imine. The mixture was washed three times with ethanol and deionized water, then dried at 50 °C in a vacuum oven. To obtain the pure Schiff-base ligand, the crude product was recrystallized from ethanol to achieve purification. For the next step, to create the target DAA@Schiff base-Pd(0) heterogenized complex, 1 gram of DAA@Schiff base was evenly spread in 20 mL of ethanol using sonication for 30 min. Following this, 0.4 gs of $Pd(OAc)_2$ were introduced into the reaction mixture. Next, 1.5 mmol of $NaBH_4$ was introduced into the reaction and stirred for an additional 24 h. Subsequently, the resulting DAA@Schiff base-Pd(0) was separated using filter paper, rinsed with n-hexane, and dried at 50 °C in an oven for 12 h (Scheme 1).

2.2. Preparation of Fe_3O_4@SiO_2@DAA@Schiff base-Pd(0)

For the synthesis of Fe_3O_4@SiO_2@DAA@Schiff base-Pd(0) MNPs, first Fe_3O_4@SiO_2 was synthesized by the co-precipitation method (Scheme 2) [22,23]. To synthesize the Fe_3O_4@SiO_2@DAA complex, 1.5 g of the prepared Fe_3O_4@SiO_2 was dispersed in 30 mL EtOH by sonication for 20 min. Then 3 mmol of 3,5-diaminobenzoic acid (DAA) was added to the reaction vessel and stirred at reflux conditions for 24 h. Following the completion of the reaction, the Fe_3O_4@SiO_2@DAA product was isolated using a neodymium magnet, followed by a thorough washing with ethyl acetate and H_2O, and subsequently dried at 60 °C in an oven for 12 h. After that, 1 gr of Fe_3O_4@SiO_2@DAA was dispersed in 50 mL of methanol and sonicated for 20 min at 30 °C. Next, 2.5 mmol of 3-hydroxybenzaldehyde was added to the flask, and the mixture was stirred under reflux conditions for 20 h. Once the reaction was complete, the mixture was allowed to cool to room temperature. The dark solid Fe_3O_4@SiO_2@DAA@Schiff base NPs were then separated from the solution using magnetic separation. Afterward, they were washed with ethyl acetate and H_2O before being dried at 50 °C in an oven for 12 h. Finally, to prepare Fe_3O_4@SiO_2@DAA@Schiff base-Pd(0) organometallic catalytic, a mixture of Fe_3O_4@SiO_2@DAA@Schiff base (1.0 g), Pd $(OAc)_2$ (3 mmol) and 35 ml ethanol was added into the flask, and it was stirred at 60 °C for 24 h. Furthermore, the reaction mixture was supplemented with 4 mmol of $NaBH_4$ and stirred for a duration of 4 h. Once the reaction was finished, the Fe_3O_4@SiO_2@DAA@Schiff base-Pd(0) catalyst was isolated, washed with water and ethanol, and then dried under vacuum.

2.3. Preparation of C-N coupling

In a 50 mL round bottom flask, iodoarene (1 mmol), Et_3N (1 mmol), arylamine (1.2 mmol), and Fe_3O_4@SiO_2@DAA@Schiff base-Pd(0) (0.03 g) were added to EtOH (3 mL) and the resultant mixture was stirred at reflux conditions. Upon the reaction completion (monitored by thin layer chromatography), the Fe_3O_4@SiO_2@DAA@Schiff base-Pd(0) was separated using a magnet, and then, EtOAc (10 mL) was added to the reaction mixture. The organic phase was separated, dried with sodium sulfate, and then the organic solvent was evaporated at room

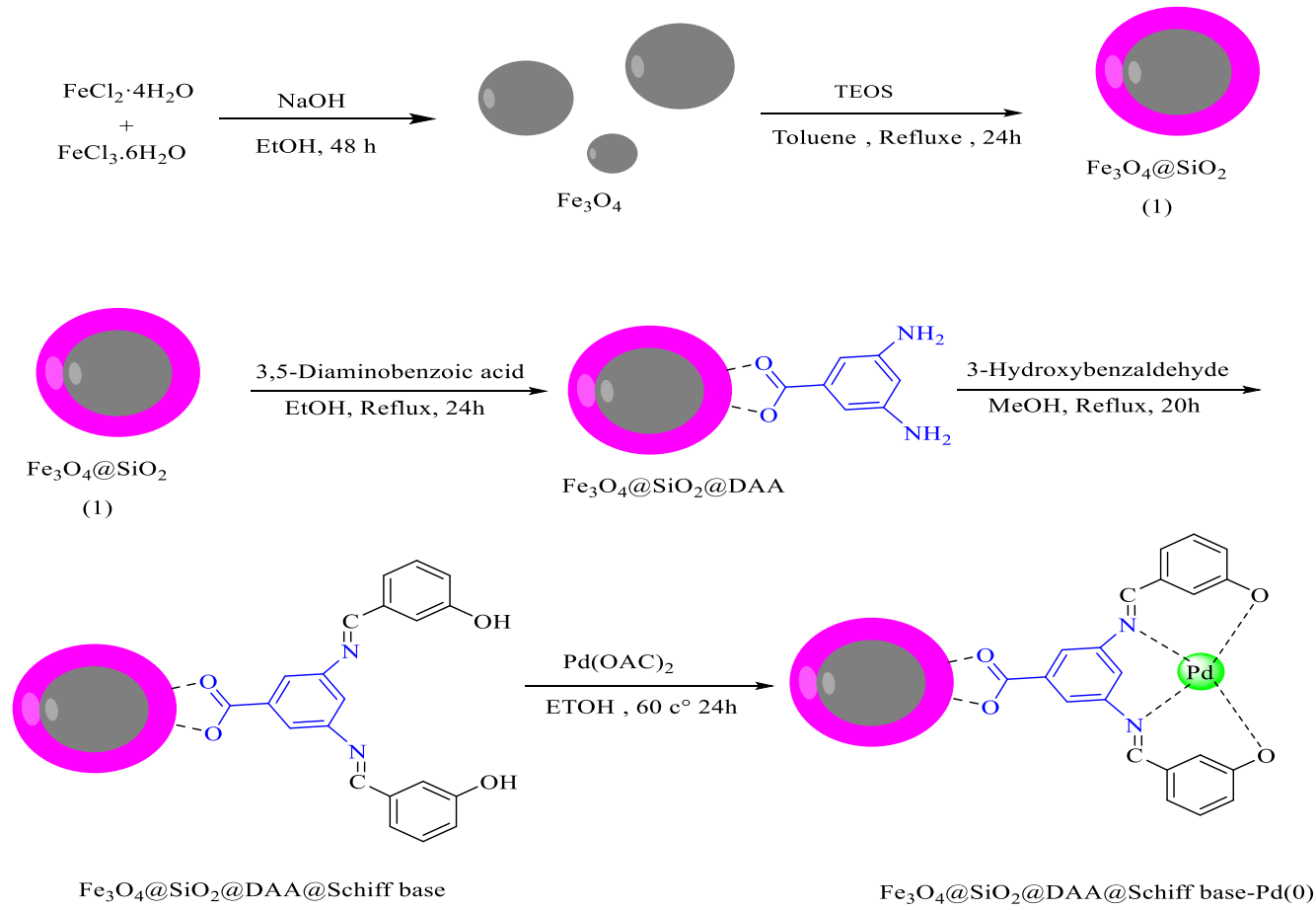

Scheme 2. Schematic diagram of Fe_3O_4@SiO_2@DAA@Schiff base-Pd(0).

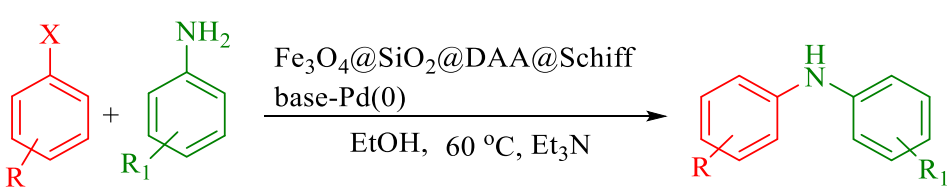

Scheme 3. Synthesis of C—N coupling reaction catalyzed by Fe_3O_4@SiO_2@DAA@Schiff base-Pd(0).

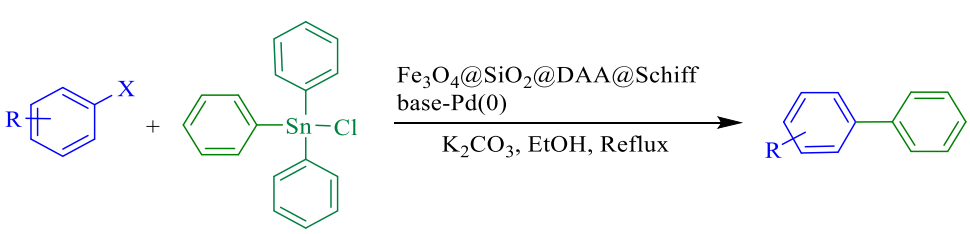

Scheme 4. Stille reaction catalyzed by Fe_3O_4@SiO_2@DAA@Schiff base-Pd(0).

temperature to obtain the saturated product with a high yield (Scheme 3).

2.4. Preparation of C-C coupling

A mixture of triphenyltin chloride (1.2 mmol), aryl halides (1 mmol), and K_2CO_3 (1.4 mmol) in the presence of Fe_3O_4@SiO_2@DAA@Schiff base-Pd(0) (0.03 g) was dissolved in ethanol and stirred at reflux condition. The reaction's progress was tracked using TLC. Once the reaction was finished, the catalyst was separated from the mixture using a magnet, and the product was washed with EtOAc and H_2O. The resulting organic layer was then dried with anhydrous sodium sulfate. After the organic solvent was evaporated, pure products were obtained as shown in Scheme 4.

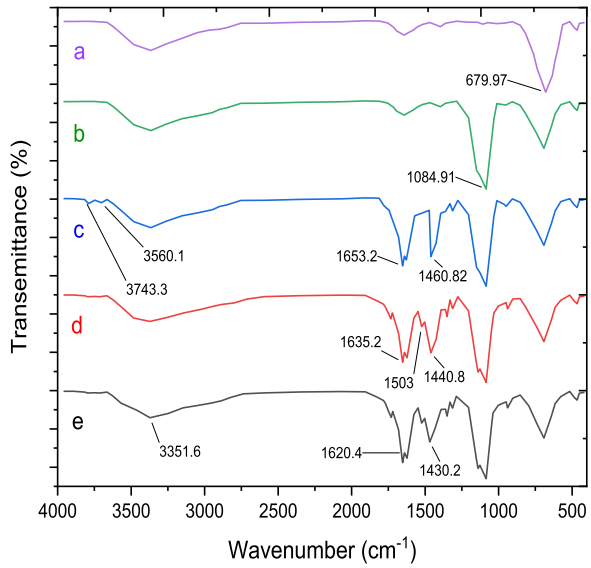

Fig. 1. Comparative study of FT-IR spectra of a) Fe_3O_4, b) Fe_3O_4@SiO_2, c) Fe_3O_4@SiO_2@DAA, d) Fe_3O_4@SiO_2@DAA@Schiff base, e) Fe_3O_4@SiO_2@-DAA@Schiff base-Pd(0).

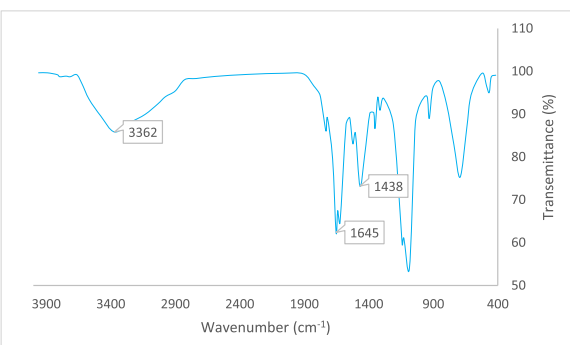

Fig. 2. FTIR analysis of recovered Fe_3O_4@SiO_2@DAA@Schiff base-Pd(0).

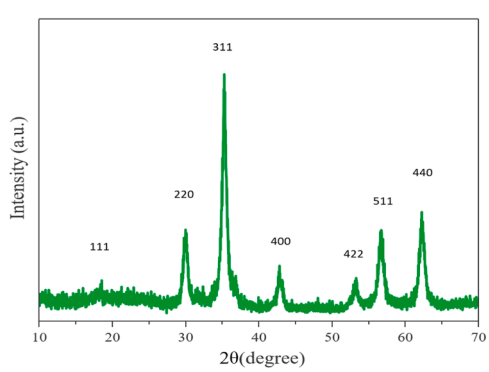

Fig. 3. XRD spectrum of Fe_3O_4@SiO_2@DAA@Schiff base-Pd(0).

2.5. Selected NMR data

[1,1′-Biphenyl] −4-carbaldehyde: ^{1}H NMR (400 MHz, DMSO): δ_H = %7.49–8.15 (m, 9H), 9.90 (s, 1H) ppm.

4-Methoxy-1,1′-biphenyl: ^{1}H NMR (400 MHz, DMSO): δ_H = 7.75 (m, 3H), 7.71 (m, 2H), 7.38 (s, 4H), 4.12 (s, 3H) ppm.

N^1-Phenylbenzene-1,4-diamine: ^{1}H NMR (400 MHz, DMSO): δ_H = 9.67 (s, 1H), 7.68 (m, 3H), 7.61 (m, 1H), 7.22 (m, 3H), 7.15 (m, 2H), 4.32 (s, 2H) ppm.

4-Methoxy-N-phenylaniline: ^{1}H NMR (400 MHz, DMSO): δ_H = 9.47 (s, 1H), 7.29 (m, 4H), 7.16 (m, 3H), 6.99 (s, 1H), 7.91 (s, 1H), 3.46 (s, 3H) ppm.

3,5-bis(((3-hydroxyphenyl)-l3-methylene)amino)benzoic acid: ^{1}H NMR (400 MHz, DMSO): δ_H = 14.03 (s, 1H), 10.23 (s, 2H), 9.40 (s, 2H),7.75 (m, 3H), 7.68 (m, 3H), 7.24 (m, 3H), 7.12 (m, 2H) ppm. M. P: 165–167 °C. HRMS (ESI): m/z $[M+H]^+$ calcd for $C_{21}H_{12}N_2O_4Pd$: M/Z 461.9823; found: M/Z:461.5197. FT-IR (KBr) (cm^{-1}): 1696 (C = N), 3000–3600 (OH). UV–Vis spectra of Pd complex: Two band appeared at 323 nm and is attributed to π→π* electronic transitions of the (aromatic rings). The second absorption band of the ligand at 380 nm may be attributed to n→π*/π→π* of imine groups.

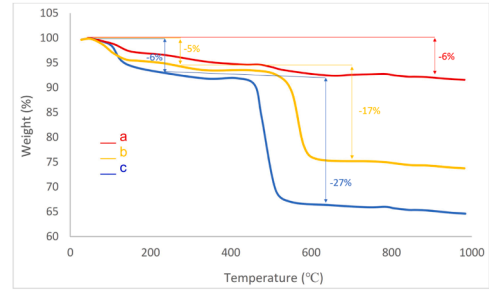

Fig. 4. TGA curve of a) Fe_3O_4, b) Fe_3O_4@SiO_2@DAA c) Fe_3O_4@SiO_2@-DAA@Schiff base-Pd(0).

3. Catalyst characterizations

The successful functionalization of the Fe_3O_4 MNPs can be understood through the use of the Fourier transform infrared (FT-IR) technique, as illustrated in Fig. 1. The absorption bands for Fe_3O_4 (Fig. 1a), and Fe_3O_4@SiO_2 (Fig. 1b) were consistent with our previous reports respectively[24–27]. The modification of Fe_3O_4@SiO_2 MNPs using DAA is confirmed by the presence of aromatic ring stretching vibrations at 1460 and 1653 cm^{-1}, as well as a broad band indicating N—H stretching mode at 3560 and 3743 cm^{-1} (Fig. 1c). Adding each layer to the previous one results in the emergence of distinct peaks corresponding to the newly introduced functional groups in the spectrum, providing evidence for the creation of a new layer (see Fig. 1d). The increased intensity of the Fe_3O_4@SiO_2@DAA@Schiff base-Pd(0) peaks notably confirms the coordination of the amino groups' nitrogen atom to Pd (refer to Fig. 1e).

Fig. 2 depicts a comparison of the FTIR spectra of the catalyst after undergoing recycling. The FTIR analysis depicted in the Fig. 2. indicates that there are no variations in the Fe_3O_4@SiO_2@DAA@Schiff base-Pd(0) after recovery, thus confirming the stability of this catalyst under reaction conditions (Fig. 2).

Fig. 3 shows the diffraction patterns of Fe_3O_4@SiO_2@DAA@Schiff base-Pd(0) NPs. A powder XRD analysis was conducted to examine the phase characteristics and crystallinity of the catalyst. The initial phases within the 2θ range of up to 30°, 36°, 45°, 54°, 57°, and 64° corresponded to the (2 2 0), (3 1 1), (4 0 0), (4 2 2), (5 1 1), and (4 4 0) planes of the highly crystalline Fe_3O_4@SiO_2@DAA@Schiff base-Pd(0) nanostructure. The XRD pattern of the catalyst indicates that the Fe_3O_4 phase remains unchanged after the modifications with a different organic functional group (Fig. 3).

Fig. 4 shows the TGA curves for Fe_3O_4, Fe_3O_4@SiO_2@DAA, and Fe_3O_4@SiO_2@DAA@Schiff base-Pd(0). Fig. 4a shows the TGA curve of Fe_3O_4, indicating that thermal decomposition took place in a single step. Below 150 °C, a reduction in weight was noticed as the physically adsorbed solvent was removed. The decrease in weight from 150 to 1000 °C is related to the oxidation of the surface hydroxides of the Fe_3O_4 magnetic nanoparticles. The TGA curve of Fe_3O_4@SiO_2@DAA is shown in Fig. 4b, which illustrates that thermal decomposition occurred in two

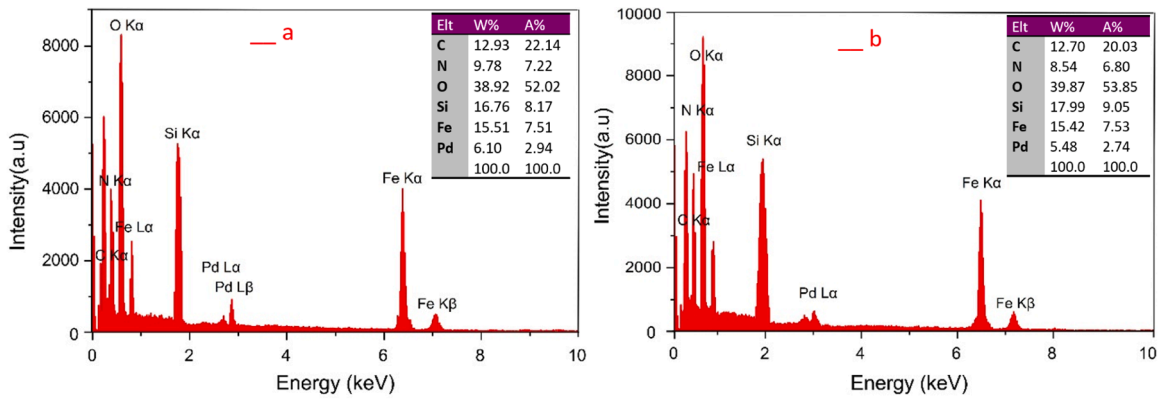

Fig. 5. EDS analysis of Fe_3O_4@SiO_2@DAA@Schiff base-Pd(0) (a) and recovered Fe_3O_4@SiO_2@DAA@Schiff base-Pd(0) (b).

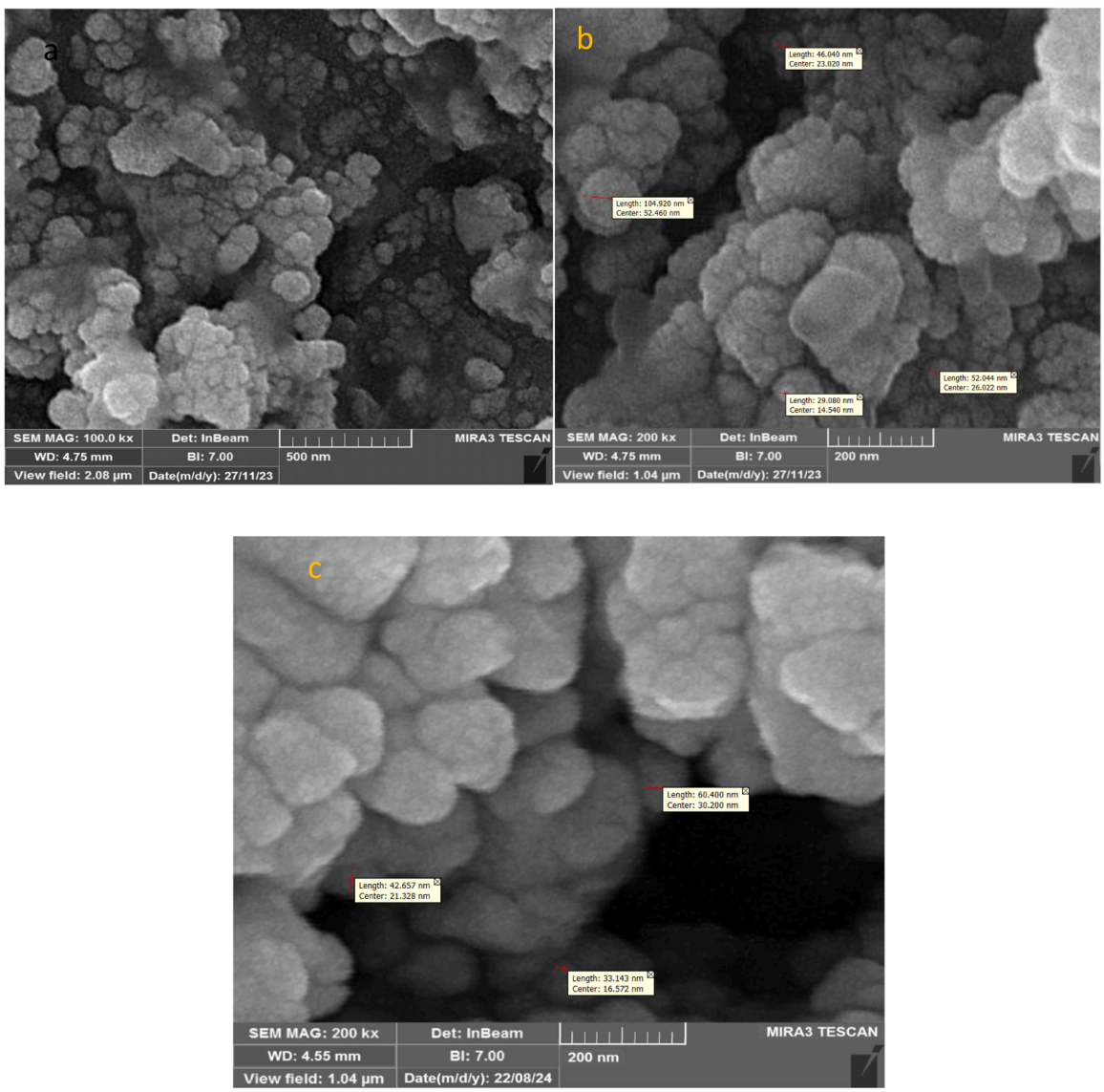

Fig. 6. SEM images of Fe_3O_4@SiO_2@DAA@Schiff base-Pd(0) (a and b) and recovered Fe_3O_4@SiO_2@DAA@Schiff base-Pd(0) (c).

steps. The initial weight loss was detected at temperatures below 150 °C, attributed to the elimination of physically adsorbed solvent. The subsequent weight loss took place between 150 °C and 700 °C, linked to the decomposition of organic groups (DAA) present on the catalyst's surface. The TGA curve of Fe_3O_4@SiO_2@DAA@Schiff base-Pd(0) indicated a weight loss of 6 % below 150 °C which corresponds to desorption of physically adsorbed solvents. The most significant weight loss, about 27 %, occurs between 150 and 600 °C and is associated with the

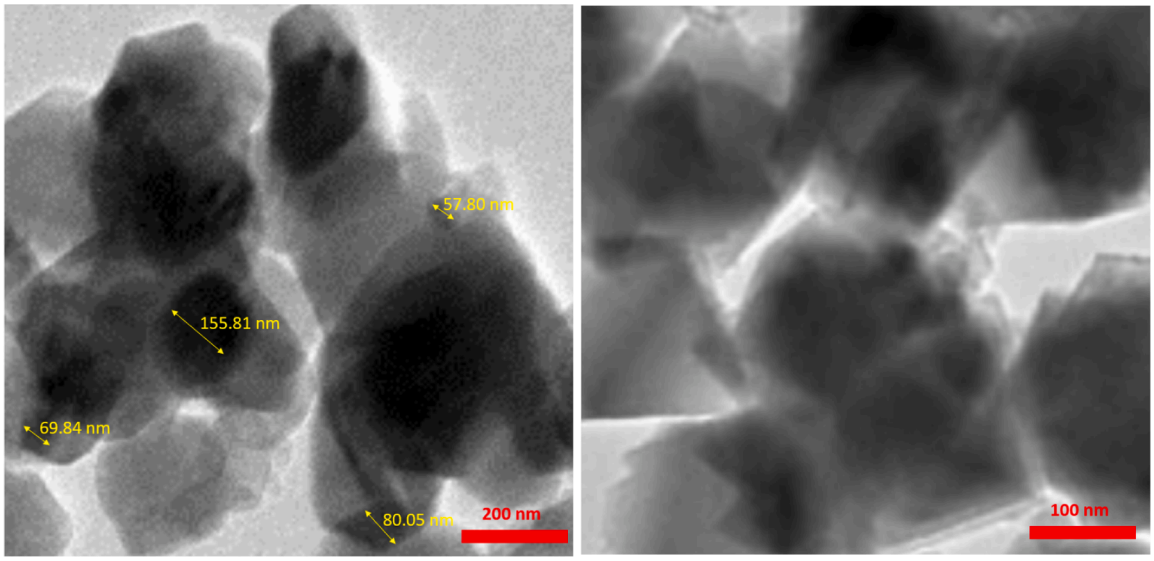

Fig. 7. TEM images of Fe_3O_4@SiO_2@DAA@Schiff base-Pd(0).

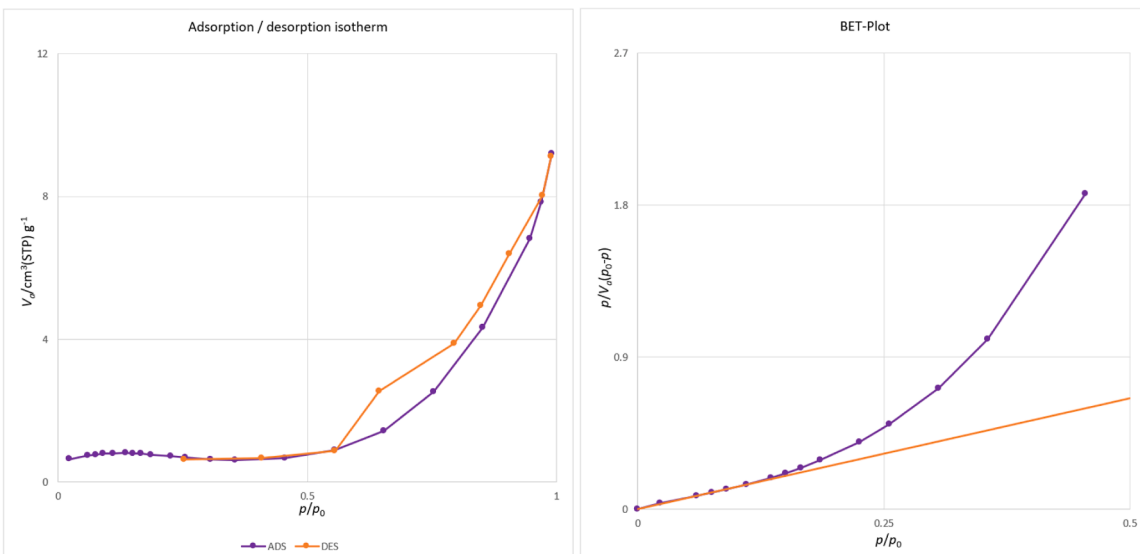

Fig. 8. Nitrogen adsorption-desorption isotherm for Fe_3O_4@SiO_2@DAA@Schiff base-Pd(0).

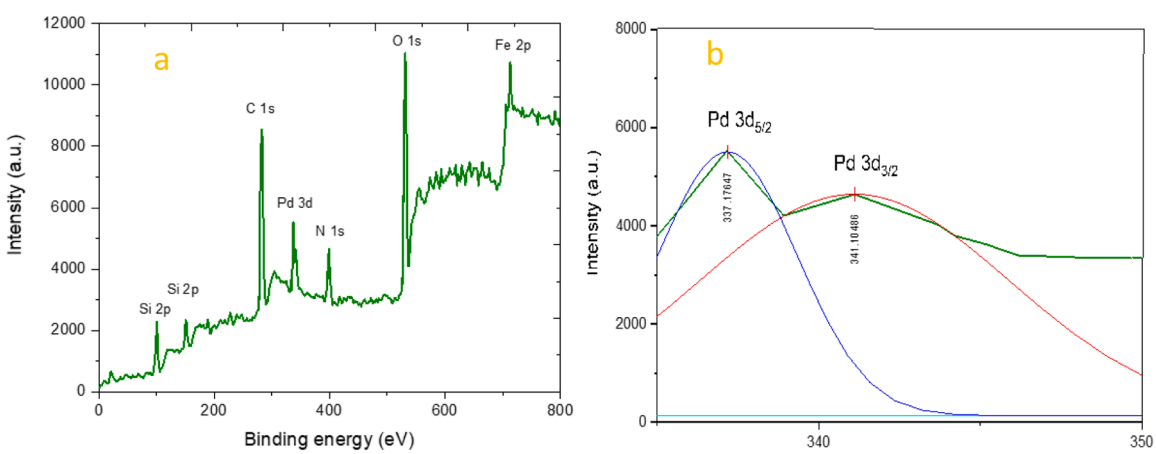

Fig. 9. XPS spectrum of Fe_3O_4@SiO_2@DAA@Schiff base-Pd(0)(a) and High-resolution XPS spectra of Pd 3d(b).

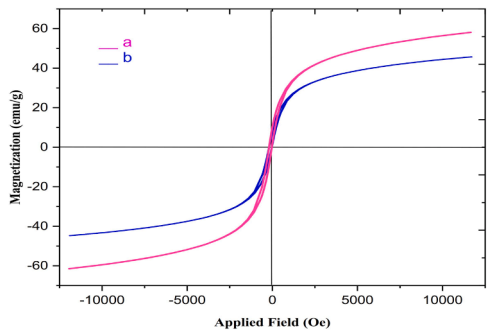

Fig. 10. VSM curves of (a) Fe_3O_4 (b) Fe_3O_4@SiO_2@DAA@Schiff base-Pd(0).

elimination of organic substances from Fe_3O_4 (see Fig. 4c).

EDX is a highly effective method for identifying the elements contained within nanoparticles and assessing their purity (see Fig. 5). Fig. 5 illustrates the EDX spectrum of Fe_3O_4@SiO_2@DAA@Schiff base-Pd(0) MNPs, confirming the presence of Fe, Si, C, O, N, and Pd in the catalyst. This substantiates the successful synthesis of the nanoparticles. Fig. 5b shows the comparison of the EDS spectrum of the catalyst after recycling. As shown, there is no change in the EDS spectrum of the catalyst after recovery.

The SEM analysis was utilized to determine the morphology and size of Fe_3O_4@SiO_2@DAA@Schiff base-Pd(0) MNPs. A SEM image of Fe_3O_4@SiO_2@DAA@Schiff base-Pd(0) MNPs reveals that the resulting nanoparticles exhibited a spherical shape, with particle sizes in the nano range (Fig. 6a and b). The SEM characterization of the recovered catalyst revealed almost identical results to those of the freshly synthesized catalyst, indicating no significant changes (Fig. 6c).

Additionally, the morphology of Fe_3O_4@SiO_2@DAA@Schiff base-Pd (0) was examined by TEM, as depicted in Fig. 7. The images show the Fe_3O_4 nanoparticles modified with DAA@Schiff base-Pd(0) forming an organic shell cover. The images obtained from scanning electron microscopy reveal that the catalyst particles have a sphere-like structure and are sized in the nanometer range. The findings were confirmed using the data obtained from transmission electron microscopy images (Fig. 7).

Porosity adsorption was employed to analyze the adsorption-desorption isotherms of N_2 at 77 °K (refer to Fig. 8). The BET method was used to assess the average pore diameter, total pore volume, and surface area of Fe_3O_4@SiO_2@DAA@Schiff base-Pd(0). Furthermore, Fig. 8 illustrates the N_2 adsorption–desorption isotherm of Fe_3O_4@-SiO_2@DAA@Schiff base-Pd(0). According to the N_2 adsorption-desorption isotherms and the BET method, the calculated surface area of Fe_3O_4@SiO_2@DAA@Schiff base-Pd(0) is 3.51 (m^2/g). Additionally, the total pore volumes and average pore diameter of Fe_3O_4@SiO_2@-DAA@Schiff base-Pd(0) were determined to be 0.014 cm^3 g^{-1} and 18 nm, respectively.

In Fig. 9, you can observe the XPS elemental survey scans and the palladium binding energy of the Fe_3O_4@SiO_2@DAA@Schiff base-Pd(0) catalyst. In Fig. 9a, peaks corresponding to oxygen, carbon, silicon, nitrogen, iron, and palladium are clearly observed in elemental survey scan. To ascertain the oxidation state of the palladium, XPS studies are carried out in Fig. 9b. The binding energy of palladium shows two distinct peaks at 341 and 337 eV, corresponding to Pd 3d3/2 and Pd 3d5/2, respectively. The peaks exhibiting binding energies of 341 and 337 eV represent the distinctive doublets indicating the spin-orbit splitting of Pd 3d 5/2 and 3d 3/2 in the metallic state (Pd0 species)[28].

Furthermore, ICP-OES analysis was conducted to determine the quantity of Pd in Fe_3O_4@SiO_2@DAA@Schiff base-Pd(0). According to the analysis, the catalyst was found to contain 2.1×10^{-4} mol of Pd per gram based on ICP-OES. Furthermore, the leaching of Pd after recycling the catalyst was investigated through ICP-OES analysis. Based on this analysis, the reutilized catalysts contain 2.0×10^{-4} mol of Pd per gram, demonstrating minimal Pd leaching from the Fe_3O_4@SiO_2@DAA@-Schiff base-Pd(0) framework.

The magnetic behavior of Fe_3O_4 (Fig. 10a), and Fe_3O_4@SiO_2@-DAA@Schiff base-Pd(0) (Fig. 10b) was investigated using VSM techniques. As anticipated, the reduction in saturation magnetization from approximately 61 emu/g to about 43 emu/g is associated with the newly applied coating layer (Fig. 10).

Catalytic studies

Buchwald-Hartwig reaction catalyzed by Fe_3O_4@SiO_2@DAA@-Schiff base-Pd

The catalytic activity of Fe_3O_4@SiO_2@DAA@Schiff base-Pd(0) was studied to determine the optimal conditions for the reaction between iodoarene and aniline, serving as a model reaction. The study examined the impact of various factors, including catalyst quantity, base

Table 1
Optimization of reaction conditions for Buchwald-Hartwig coupling reaction of arylamine with iodoarene.

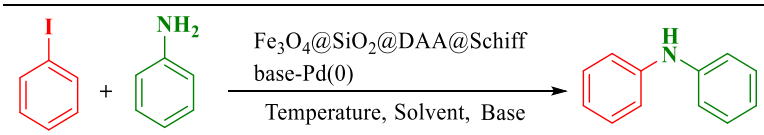

Entry	Catalyst (g)	Solvent	Base	Temp. (°C)	Time (h)	Isolated yield (%)
1	–	EtOH	Et_3N	Reflux	10	–
2	0.01	EtOH	Et_3N	Reflux	1.5	35
3	0.015	EtOH	Et_3N	Reflux	1.5	61
4	0.02	EtOH	Et_3N	Reflux	1.5	82
5	0.03	EtOH	Et_3N	Reflux	1.5	97
6	0.035	EtOH	Et_3N	Reflux	1.5	97
7	0.03	PEG	Et_3N	100	1.5	65
8	0.03	DMSO	Et_3N	Reflux	1.5	N.R
9	0.03	H_2O	Et_3N	80	1.5	45
10	0.03	H_2O/ EtOH	Et_3N	Reflux	1.5	70
11	0.03	EtOH	NaOH	Reflux	1.5	55
12	0.03	EtOH	K_2CO_3	Reflux	1.5	69
13	0.03	EtOH	–	Reflux	1.5	25
14	0.03	EtOH	Et_3N	R. T	3	55
15	0.03	EtOH	Et_3N	50	1.5	73
16	0.03	EtOH	Et_3N	60	1.5	89
17	0.03	EtOH	Et_3N	70	1.5	94

Table 2
Fe_3O_4@SiO_2@DAA@Schiff base-Pd(0) catalyzed Buchwald-Hartwig reaction of various halides with amines.

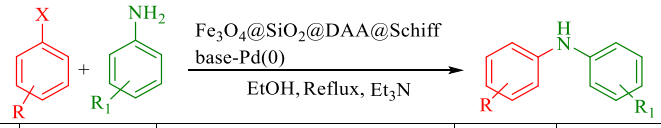

Entry	Aryl halide	Arylamine	Product	Time (h)	Yield (%) [a,b]	TON	TOF (h^{-1})
1	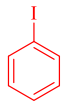	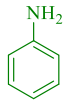	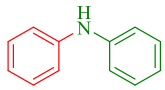	2	94	15.6	7.8
2	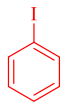	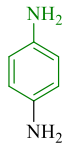	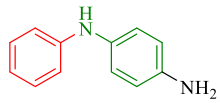	3	98	16.3	5.43
3	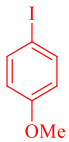	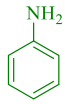	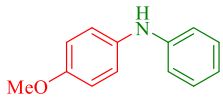	2.5	93	15.5	6.2
4	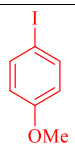	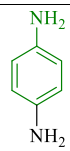	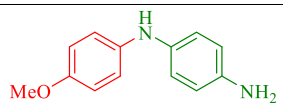	1.5	93	15.5	10.1
5	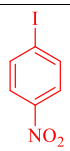	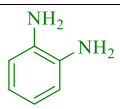	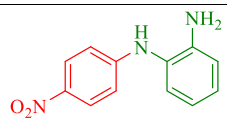	5	75	12.5	2.5
6	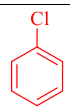	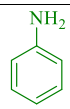	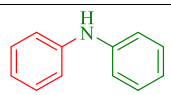	4	94	15.6	3.9
7	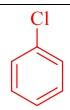	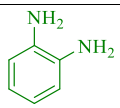	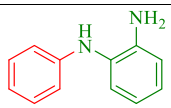	3	93	15.5	5.6
8	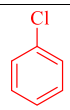	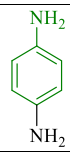	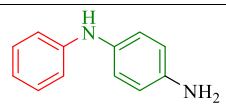	2.5	92	15.3	6
9	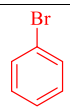	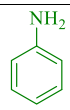	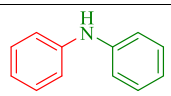	2	90	15	7.5
11	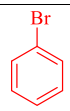	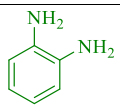	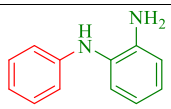	2	92	15.3	7.6
12	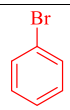	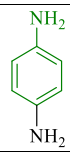	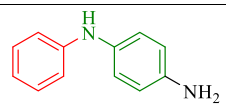	3	94	15.6	5.2

[a]Isolated yield.
[b]Reaction conditions: arylamine (1.2 mmol), aryl halide (1 mmol), Fe_3O_4@SiO_2@DAA@Schiff base-Pd(0) (0.03 g), Et_3N (1 mmol), in EtOH (3 ml) at reflux condition.

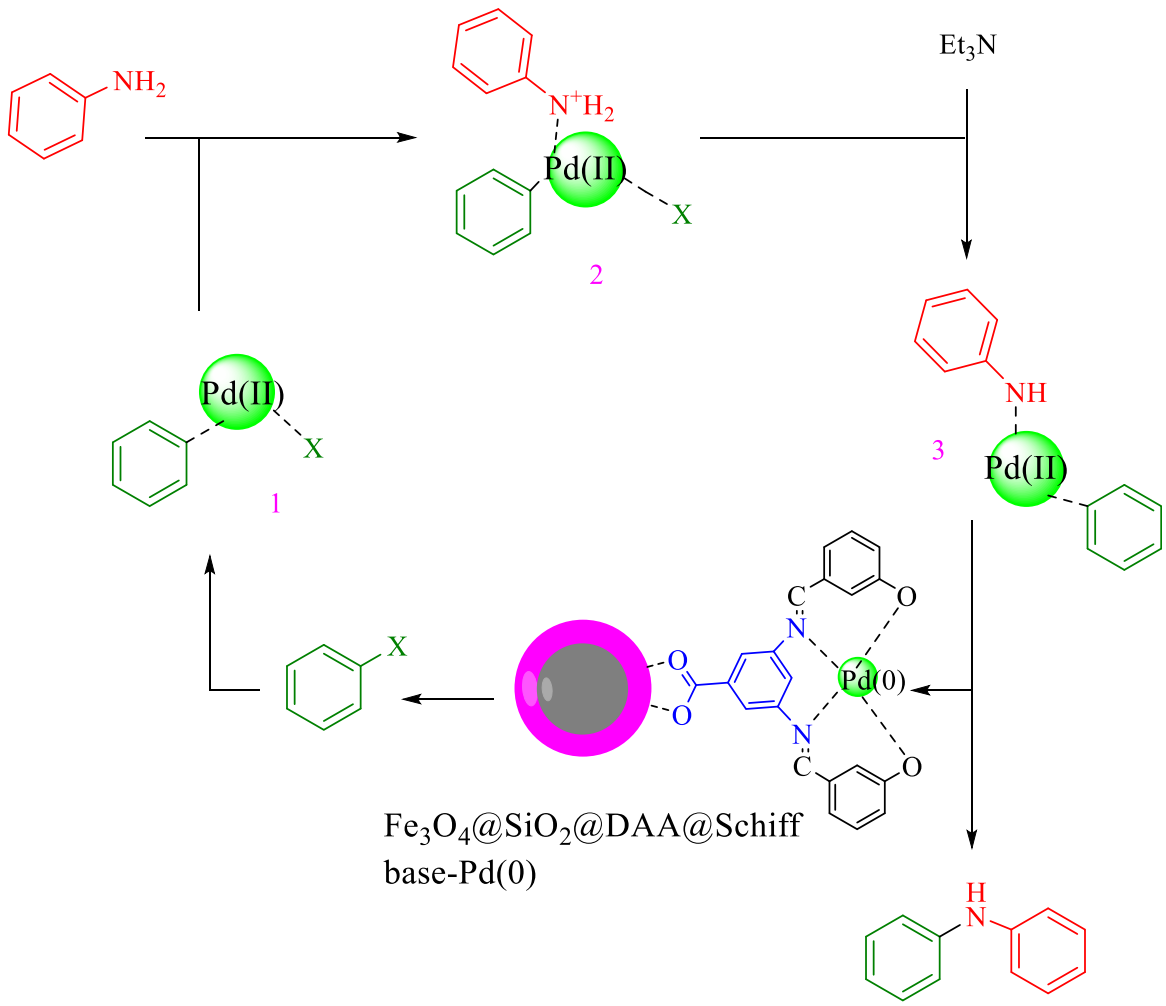

Scheme 5. Possible mechanism for C—N coupling reaction.

Table 3
Optimization of the reaction conditions for the coupling reaction of iodobenzene with triphenyl tin chloride in the presence of Fe_3O_4@SiO_2@DAA@Schiff base-Pd(0).

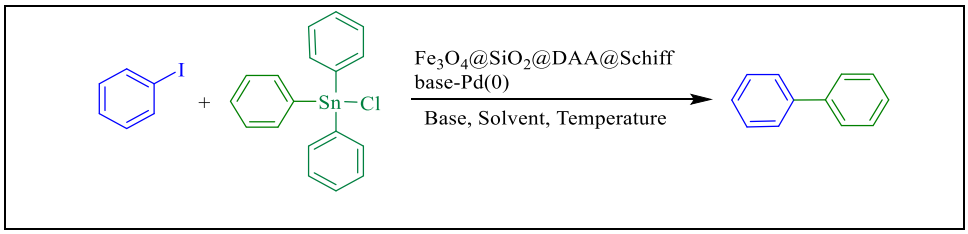

Entry	Catalyst (g)	Solvent	Base	Temperature (°C)	Time (min)	Yield (%)[a]
1	–	EtOH	K_2CO_3	60	1 days	N. R
2	0.005	EtOH	K_2CO_3	60	20	53
3	0.01	EtOH	K_2CO_3	60	20	82
4	0.02	EtOH	K_2CO_3	60	20	93
5	0.03	EtOH	K_2CO_3	60	20	98
6	0.035	EtOH	K_2CO_3	60	20	98
7	0.03	H_2O	K_2CO_3	60	20	35
8	0.03	hexane	K_2CO_3	60	20	48
9	0.03	Acetonitrile	K_2CO_3	60	20	75
10	0.03	EtOAc	K_2CO_3	60	20	82
11	0.03	MeOH	K_2CO_3	60	20	92
12	0.03	EtOH	*t*-BuOK	60	20	90
13	0.03	EtOH	Na_2CO_3	60	20	85
14	0.03	EtOH	Cs_2CO_3	60	20	88
15	0.03	EtOH	Et_3N	60	20	82
16	0.03	EtOH	NaOH	60	20	40
17.	0.03	EtOH	KOH	60	20	30

concentration, different solvents, and temperature, on the outcome of the reaction. The reaction progress was monitored using TLC. Once the reaction was complete, the product was extracted using ethyl acetate as the solvent. Also, the reaction showed the best response in EtOH solvent under reflux conditions with Et_3N as the base in the presence of 0.03 g of Fe_3O_4@SiO_2@DAA@Schiff base-Pd(0) (Table 1).

The optimized reaction condition on hand, the Buchwald-Hartwig reaction of different amines with different aryl halide derivatives was examined. First, different substituted aryl halides containing NO_2, $COCH_3$, with amines were investigated. The results clearly showed that the reaction can be completed in 1.5–5 h with moderate to excellent yields for both electron-withdrawing and electron-donating substituted amines and different aryl halides (Table 2).

Scheme 5 illustrates the proposed mechanism for the C–N cross-coupling reaction, building on prior studies. The process starts with the oxidative addition of aryl halide to Pd, yielding intermediate (1). Subsequently, intermediate (1) interacts with aryl amine in the presence of the base Et_3N to yield intermediate (2). Finally, reductive elimination of intermediate (2) produces the desired product and releases the Fe_3O_4@SiO_2@DAA@Schiff base-Pd(0) nanoparticle.

In early research, the Fe_3O_4@SiO_2@DAA@Schiff base-Pd(0) complex was then utilized as catalyst for the Stille reaction. The first experiments involved using 1 mmol of iodobenzene as the substrate to optimize the reaction conditions, including the quantity of catalysts, solvents, and base (refer to Table 3). Initially, the impact of varying quantities of the nanocatalyst on the reaction's results was examined. It was found that the optimum yield was achieved when 0.03 g of Fe_3O_4@SiO_2@DAA@Schiff base-Pd(0) was present. Following that, we proceeded to assess the impact of the base, solvent, and reaction temperature, resulting in the identification of ethanol as the optimal medium for achieving the highest yield of biphenyl product at 60 °C, with potassium carbonate emerging as the most effective base. According to the observed results, the optimal conditions for this reaction are Fe_3O_4@SiO_2@DAA@Schiff base-Pd(0) catalyst (0.03 g) and potassium carbonate (2 mmol) as the base in the ethanol at 60 °C.

With the optimized reaction conditions at our disposal, the substrate scope of the triphenyltin chloride and aryl halides was studied in the presence of potassium carbonate and 0.03 g of Fe_3O_4@SiO_2@DAA@-Schiff base-Pd(0) in ethanol at 60 °C, and the results are summarized in Table 4. A variety of aryl halides with both electron-donating and electron-withdrawing groups efficiently reacted with triphenyltin chloride, resulting in excellent isolated yields and high TOF values as shown in Table 4.

For a more in-depth exploration of the mechanism of action of Pd NPs in coupling reactions, a potential mechanism for Stille coupling using Fe_3O_4@SiO_2@DAA@Schiff base-Pd(0) was outlined in Scheme 6. The process begins with the oxidative addition of aryl halides to Fe_3O_4@SiO_2@DAA@Schiff base-Pd(0), leading to the formation of the Pd complex and intermediate 2. Subsequently, transmetalation takes place as an organotin reagent reacts with intermediate 2, yielding intermediate 3. Ultimately, the reductive elimination of intermediate 3 results in the production of biaryl product and Fe_3O_4@SiO_2@DAA@-Schiff base-Pd(0) (Scheme 6). In the presence of the DAA@Schiff base ligand, EtOH as a solvent, and a base (K_2CO_3), it is plausible that stable anionic complexes [Schiff base-Pd(0)] are generated, consequently expediting the oxidative addition of aryl halides with ph_3SnCl (Scheme 6).

4. Recyclability of Fe_3O_4@SiO_2@DAA@Schiff base-Pd(0)

The potential for Fe_3O_4@SiO_2@DAA@Schiff base-Pd(0) to be recycled was investigated in the optimized synthesis of biphenyl. The catalyst was used repeatedly for up to five cycles without experiencing any notable decline in its catalytic effectiveness or palladium release (see Fig. 11).

The efficiency of Fe_3O_4@SiO_2@DAA@Schiff base-Pd(0) as nanocatalyst was considered by comparing these obtained results with previously reported nanocatalysts in the authentic literature (Table 5). Results for Stille reaction from coupling reaction of iodobenzene with triphenyltin chloride in the presence of Fe_3O_4@SiO_2@DAA@Schiff base-Pd(0) and previously reported catalysts are summarized in Table 5. The Nano-Fe_3O_4@SiO_2@DAA@Schiff base-Pd(0) catalyst offers several advantages, including reduced reaction times, simplified product purification, high yields, low reaction temperature, easy catalyst recovery,

Table 4
Catalytic coupling reaction of various aryl halides with triphenyl tin chloride in the presence of catalytic amounts of Fe_3O_4@SiO_2@DAA@Schiff base-Pd(0).

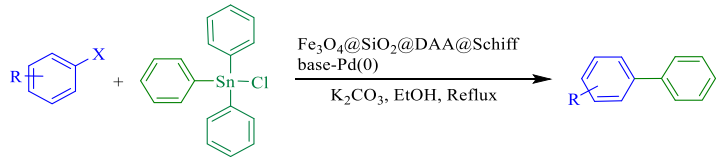

Entry	Aryl halide	Product	Time (min)	Yield (%)[a]	TON	TOF (min^{-1})
1		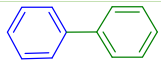	20	98	16.3	54.3
2	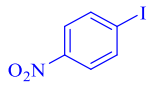	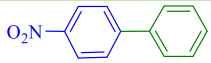	50	93	15.5	18.67
3	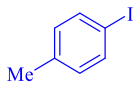	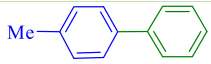	40	95	15.8	26.3
4	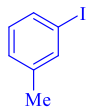	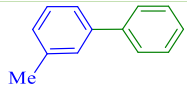	30	94	15.6	31.2
5	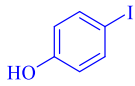	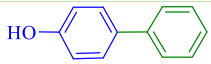	15	91	15.1	60.4
6	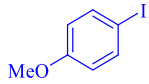	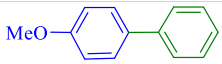	20	90	15	50
7	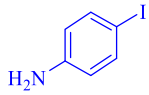	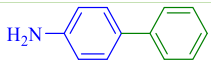	30	96	16	32
8	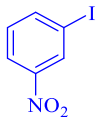	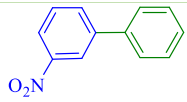	35	96	16	27.5
9	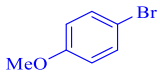	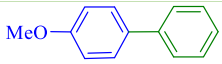	15	95	18.8	75.2
10	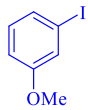	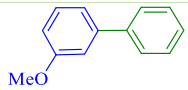	25	96	16	28
11	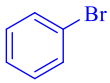	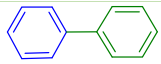	35	91	15.1	26

(*continued on next page*)

Table 4 (*continued*)

12	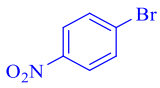	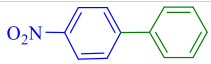	25	93	15.5	37.8
13	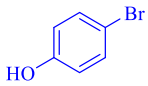	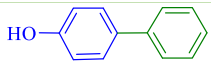	15	92	15.3	61.2
14	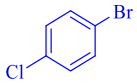	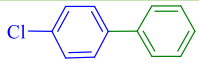	60	91	15.1	15.1
15	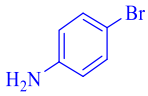	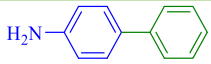	65	94	15.6	14.8
16		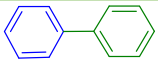	30	92	15.3	7.6
17	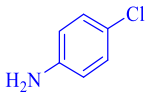	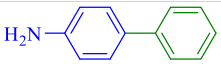	110	85	14.1	7.83
18	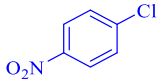	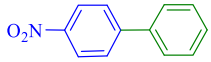	40	95	15.8	26.3
19	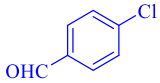	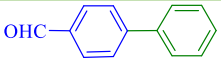	55	75	12.5	13.4
20	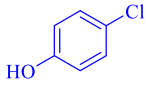	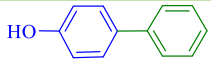	80	90	15	11.5

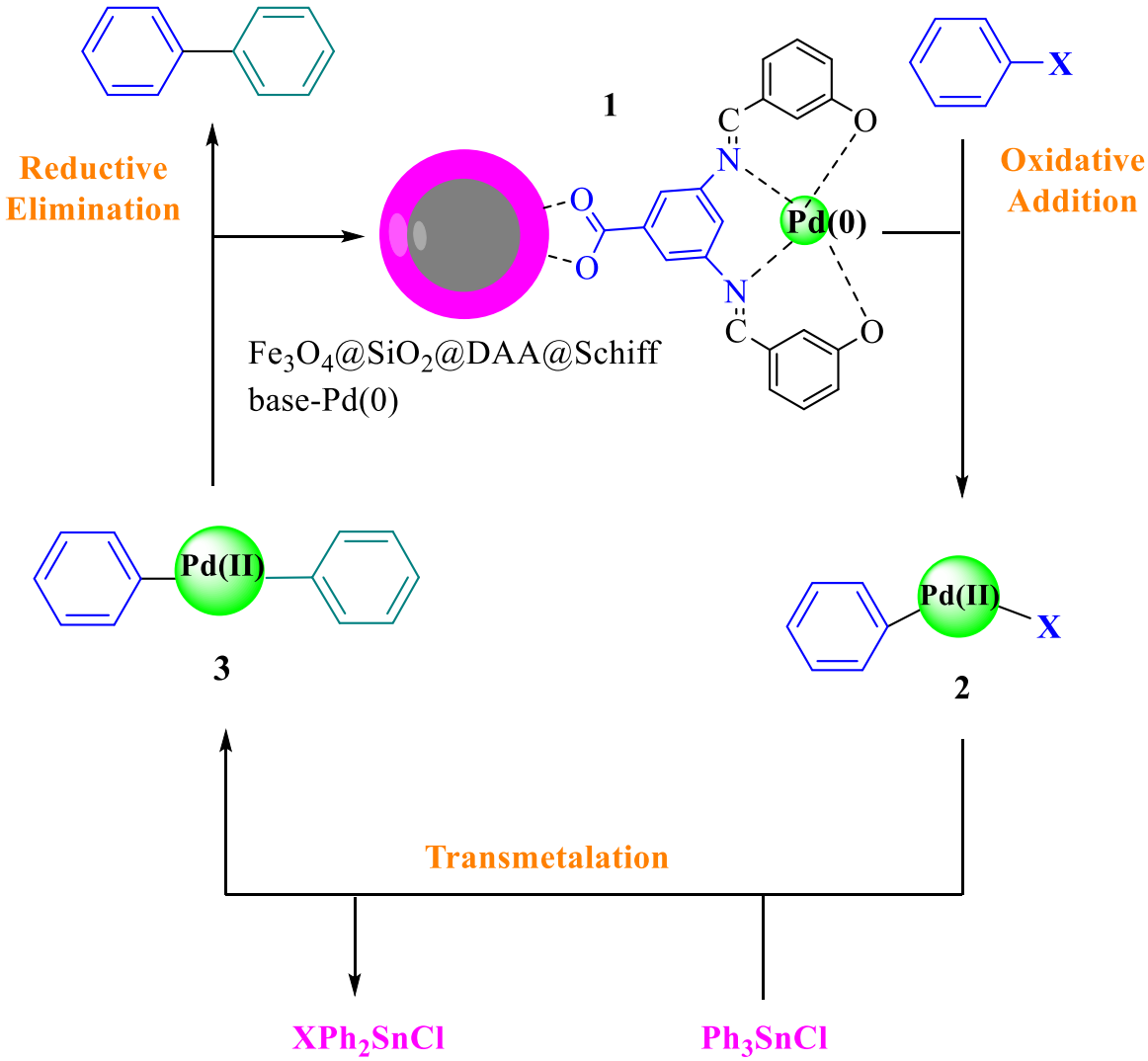

Scheme 6. Possible mechanism for Stille reaction.

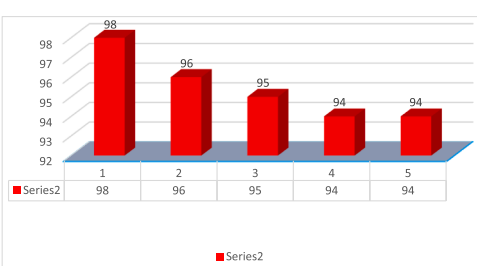

Fig. 11. Recyclability of Fe_3O_4@SiO_2@DAA@Schiff base-Pd(0) in the synthesis of Stille reaction.

and the use of environmentally friendly solvents. Fe_3O_4@SiO_2@-DAA@Schiff base-Pd(0) is an efficient catalyst, valuable for organic reactions and the synthesis of organic compounds.

5. Conclusion

We have effectively created and produced magnetic core-shell Fe_3O_4@SiO_2 nanoparticles functionalized by DAA@Schiff base-Pd(0) complex, which serve as an innovative reusable catalyst for C—N and C—C cross-coupling reactions. Furthermore, this new Fe_3O_4@SiO_2@-DAA@Schiff base-Pd(0) can be readily prepared from commercially available materials. The prepared catalyst, Fe_3O_4@SiO_2@DAA@Schiff base-Pd(0), was identified via FT-IR, ICP-OES, EDS, TEM, SEM, TGA, XRD, BET, XPS, and VSM techniques. This method is notable for its straightforward procedures, rapid reaction times, high yields, efficient magnetic separation, clean reaction profiles, low catalyst loading, easy product separations, and the good chemical stability of the catalyst.

Table 5
Comparing catalytic activity of Fe_3O_4@SiO_2@DAA@Schiff base-Pd(0) with previously reported methods in the C—C coupling reaction.

Entry	Catalyst	Condition reaction	product	Yield (%)	Ref.
1.	Pd@BTU-GO	NaOAc, PEG-400, 25 °C	Biphenyl	94	[29]
2.	Pd/chamomile@Fe_3O_4	K_2CO_3, EtOH: H_2O, 60 °C	Biphenyl	96	[30]
3.	Pd NPs/C@Fe_3O_4	DMF, K_2CO_3, 100 °C	Biphenyl	95	[31]
4.	Fe_3O_4@SiO_2@DAA@Schiff base-Pd(0)	EtOH, K_2CO_3, 60 °C	Biphenyl	98	This work

CRediT authorship contribution statement

Durgesh Singh: Investigation, Funding acquisition, Formal analysis. **Kamini Singh:** Writing – original draft, Visualization, Validation. **Vicky Jain:** Validation, Software, Resources, Project administration. **Subbulakshmi Ganesan:** Writing – review & editing, Writing – original draft, Resources. **Junainah Abd Hamid:** Resources, Project administration, Methodology, Data curation, Conceptualization. **Mamata Chahar:** Writing – review & editing, Validation, Software, Methodology, Investigation. **Suman Saini:** Methodology, Investigation, Funding acquisition. **Munther Kadhim Abosaoda:** Resources, Project administration, Methodology. **M. Atif:** Project administration, Methodology, Investigation. **Mohammed A. El-Meligy:** Validation, Supervision, Software, Methodology, Investigation.

Declaration of competing interest

The authors declare that they have no known competing financial interests or personal relationships that could have appeared to influence the work reported in this paper.

Data availability

All data generated or analyzed during this study are included in this published article and its supplementary information files.

Acknowledgements

The authors present their appreciation to King Saud University for funding this research through Researchers Supporting Program number (RSP2024R397), King Saud University, Riyadh, Saudi Arabia.

Supplementary materials

Supplementary material associated with this article can be found, in the online version, at doi:10.1016/j.molstruc.2024.140241.

References

[1] M.A. Ashraf, Z. Liu, C. Li, D. Zhang, Fe3O4@HcdMeen-Pd(0) organic–inorganic hybrid: as a novel heterogeneous nanocatalyst for chemo and homoselective heck C–C cross-coupling synthesis of butyl cinnamates, Catal Lett. (2021), https://doi.org/10.1007/s10562-020-03509-0.

[2] A. Taheri Kal Koshvandi, M.M. Heravi, T. Momeni, Current applications of Suzuki–Miyaura coupling reaction in the total synthesis of natural products: an update, Appl. Organomet. Chem. 32 (2018) e4210, https://doi.org/10.1002/aoc.4210.

[3] Z. Chen, E. Vorobyeva, S. Mitchell, E. Fako, M.A. Ortuño, N. López, S.M. Collins, P. A. Midgley, S. Richard, G. Vilé, J. Pérez-Ramírez, A heterogeneous single-atom palladium catalyst surpassing homogeneous systems for Suzuki coupling, Nat. Nanotechnol. 13 (2018) 702–707, https://doi.org/10.1038/s41565-018-0167-2.

[4] M.A. Ashraf, Z. Liu, D. Zhang, A. Alimoradi, L-lysine-Pd Complex Supported on Fe 3 O 4 MNPs: a novel recoverable magnetic nanocatalyst for Suzuki C-C cross-coupling reaction, Appl. Organomet. Chem. 34 (2020) e5668, https://doi.org/10.1002/aoc.5668.

[5] V. Kandathil, A. Siddiqa, A. Patra, B. Kulkarni, M. Kempasiddaiah, B.S. Sasidhar, S. A. Patil, C.S. Rout, S.A. Patil, NHC-Pd complex heterogenized on graphene oxide for cross-coupling reactions and supercapacitor applications, Appl. Organomet. Chem. 34 (2020), https://doi.org/10.1002/aoc.5924.

[6] U.S. Kanchana, E.J. Diana, T.V. Mathew, G. Anilkumar, Palladium-catalyzed cross-coupling reactions of coumarin derivatives: an overview, Appl. Organomet. Chem. 34 (2020), https://doi.org/10.1002/aoc.5983.

[7] J. Lakshmidevi, B.R. Naidu, K. Venkateswarlu, CuI in biorenewable basic medium: three novel and low E-factor Suzuki-Miyaura cross-coupling reactions, Mol. Catal. 522 (2022) 112237, https://doi.org/10.1016/j.mcat.2022.112237.

[8] S. Gorji, R. Ghorbani-Vaghei, Ag nanoparticles stabilized on basalt fibers as a novel, stable, and reusable catalyst for Suzuki–Miyaura coupling reactions, Appl. Organomet. Chem. 35 (2021), https://doi.org/10.1002/aoc.6018.

[9] H. Azizollahi, H. Eshghi, J.-A. García-López, Fe3O4-SAHPG-Pd0 nanoparticles: a ligand-free and low Pd loading quasiheterogeneous catalyst active for mild Suzuki–Miyaura coupling and C-H activation of pyrimidine cores, Appl. Organomet. Chem. 35 (2021), https://doi.org/10.1002/aoc.6020.

[10] V.V. Gaikwad, P.A. Mane, S. Dey, B.M. Bhanage, Xantphos-ligated palladium dithiolates: an unprecedented and convenient catalyst for the carbonylative Suzuki–Miyaura cross-coupling reaction with high turnover number and turnover frequency, Appl. Organomet. Chem. 34 (2020), https://doi.org/10.1002/aoc.5255.

[11] Y. Lei, W. Zhu, Y. Wan, R. Wang, H. Liu, Pd nanoparticles supported on amphiphilic porous organic polymer as an efficient catalyst for aqueous hydrodechlorination and Suzuki-Miyaura coupling reactions, Appl. Organomet. Chem. 34 (2020), https://doi.org/10.1002/aoc.5364.

[12] J. Chen, J. Zhang, Y. Zhang, M. Xie, T. Li, Nanoporous phenanthroline polymer locked Pd as highly efficient catalyst for Suzuki-Miyaura Coupling reaction at room temperature, Appl. Organomet. Chem. 34 (2020), https://doi.org/10.1002/aoc.5310.

[13] M.S. Asgari, P. Rashidi Ranjbar, R. Rahimi, M. Mahdavi, Synthesis of arylidene – isoquinolinones bearing combretastatin skeleton by cyclocarbopalladation/cross coupling tandem Heck-Suzuki Miaura reactions using nano catalyst Pd@Py-IL-SPION, Appl. Organomet. Chem. 34 (2020), https://doi.org/10.1002/aoc.5279.

[14] S.R. Aabaka, J. Mao, M. Lavanya, K. Venkateswarlu, Z. Huang, J. Mao, X. Yang, C. Lin, Nanocellulose supported PdNPs as in situ formed nano catalyst for the suzuki coupling reaction in aqueous media: a green approach and waste to wealth, J. Organomet. Chem. 937 (2021) 121719, https://doi.org/10.1016/j.jorganchem.2021.121719.

[15] C. Han, R. Qi, R. Sun, K. Fan, B. Johannessen, D.-C. Qi, S. Cao, J. Xu, Enhanced support effects in single-atom copper-incorporated carbon nitride for photocatalytic suzuki cross-coupling reactions, Appl. Catal. B 320 (2023) 121954, https://doi.org/10.1016/j.apcatb.2022.121954.

[16] C.-J. Li, Reflection and perspective on green chemistry development for chemical synthesis - Daoist insights, Green Chem. 18 (2016) 1836–1838, https://doi.org/10.1039/c6gc90029a.

[17] C.C.C. Johansson Seechurn, M.O. Kitching, T.J. Colacot, V. Snieckus, Palladium-catalyzed cross-coupling: a historical contextual perspective to the 2010 nobel prize, Angew. Chem. Int. Ed. 51 (2012) 5062–5085, https://doi.org/10.1002/anie.201107017.

[18] S. Zhu, H. Li, Y. Li, Z. Huang, L. Chu, Exploring visible light for carbon–nitrogen and carbon–oxygen bond formation via nickel catalysis, Org. Chem. Front. 10 (2023) 548–569, https://doi.org/10.1039/D2QO01700H.

[19] S.B. Mohite, M. Bera, V. Kumar, R. Karpoormath, S.B. Baba, A.S. Kumbhar, O-Benzoylhydroxylamines: a versatile electrophilic aminating reagent for transition metal-catalyzed C–N bond-forming reactions, Top. Curr. Chem. 381 (2022) 4, https://doi.org/10.1007/s41061-022-00414-5.

[20] N. Muniyappan, S. Sabiah, Synthesis, structure, and characterization of picolyl- and benzyl-linked biphenyl palladium N-heterocyclic carbene complexes and their catalytic activity in acylative cross-coupling reactions, Appl. Organomet. Chem. 34 (2020), https://doi.org/10.1002/aoc.5421.

[21] H. Alamgholiloo, S. Rostamnia, N. Noroozi Pesyan, Extended architectures constructed of thiourea-modified SBA-15 nanoreactor: a versatile new support for the fabrication of palladium pre-catalyst, Appl. Organomet. Chem. 34 (2020), https://doi.org/10.1002/aoc.5452.

[22] F. Zhang, B. Shen, W. Jiang, H. Yuan, H. Zhou, Hydrolysis extraction of diosgenin from Dioscorea nipponica Makino by sulfonated magnetic solid composites, J. Nanopart. Res. 21 (2019), https://doi.org/10.1007/s11051-019-4702-3.

[23] I. Dindarloo Inaloo, S. Majnooni, H. Eslahi, M. Esmaeilpour, N-Arylation of (hetero)arylamines using aryl sulfamates and carbamates via C–O bond activation enabled by a reusable and durable nickel(0) catalyst, New J. Chem. 44 (2020) 13266–13278, https://doi.org/10.1039/D0NJ01610A.

[24] A.H. Gemeay, B.E. Keshta, R.G. El-Sharkawy, A.B. Zaki, Chemical insight into the adsorption of reactive wool dyes onto amine-functionalized magnetite/silica core-shell from industrial wastewaters, Environ. Sci. Poll. Res. 27 (2020) 32341–32358, https://doi.org/10.1007/s11356-019-06530-y.

[25] P. Gupta, S. Rani, D. Sah, J.Shabir Surabhi, B. Singh, B. Pani, S. Mozumdar, Basic ionic liquid grafted on magnetic nanoparticles: an efficient and highly active recyclable catalyst for the synthesis of β-nitroalcohols and 4H-benzo[b]pyrans, J. Mol. Struct. 1274 (2023) 134351, https://doi.org/10.1016/j.molstruc.2022.134351.

[26] I. Dindarloo Inaloo, S. Majnooni, H. Eslahi, M. Esmaeilpour, Air-stable Fe3O4@SiO2-EDTA-Ni(0) as an efficient recyclable magnetic nanocatalyst for effective Suzuki-Miyaura and heck cross-coupling via aryl sulfamates and carbamates, Appl. Organomet. Chem. 34 (2020) e5662, https://doi.org/10.1002/aoc.5662.

[27] M.A. Zolfigol, M. Navazeni, M. Yarie, R. Ayazi-Nasrabadi, Application of Fe3O4@SiO2/(CH2)3-[imidazolium-SO3H]Cl as a robust, magnetically recoverable solid acid catalyst for the facile preparation of arylbispyranylmethanes, Can. J. Chem. 95 (2017) 1248–1252, https://doi.org/10.1139/cjc-2017-0232.

[28] Y. Tuo, G. Liu, B. Dong, J. Zhou, A. Wang, R. Jin, H. Lv, Z. Dou, W. Huang, Microbial synthesis of Pd/Fe3O4, Au/Fe3O4 and PdAu/Fe3O4 nanocomposites for catalytic reduction of nitroaromatic compounds, Sci. Rep. 5 (2015) 13515, https://doi.org/10.1038/srep13515.

[29] H. Alamgholiloo, S. Rostamnia, N.N. Pesyan, Anchoring and stabilization of colloidal PdNPs on exfoliated bis-thiourea modified graphene oxide layers with super catalytic activity in water and PEG, Colloids Surf. A 602 (2020) 125130, https://doi.org/10.1016/j.colsurfa.2020.125130.

[30] H. Veisi, A. Zohrabi, S.A. Kamangar, B. Karmakar, S.G. Saremi, K. Varmira, M. Hamelian, Green synthesis of Pd/Fe3O4 nanoparticles using chamomile extract as highly active and recyclable catalyst for Suzuki coupling reaction, J. Organomet. Chem. 951 (2021), https://doi.org/10.1016/j.jorganchem.2021.122005.

[31] B.S. Kumar, R. Anbarasan, A.J. Amali, K. Pitchumani, Isolable C@Fe3O4 nanospheres supported cubical Pd nanoparticles as reusable catalysts for Stille and Mizoroki-Heck coupling reactions, Tetrahedron Lett. 58 (2017) 3276–3282, https://doi.org/10.1016/j.tetlet.2017.07.025.